Title

CD36 Repression Activates a Multicellular Stromal Program Shared by High Mammographic Density and Tumor Tissues

Journal

Cancer Discovery, 2(9)

ISSN

2159-8274

Authors

DeFilippis, Rosa Anna
Chang, Hang
Dumont, Nancy
et al.

Publication Date

2012-09-01

DOI

10.1158/2159-8290.cd-12-0107

Peer reviewed

Published OnlineFirst July 9, 2012; DOI: 10.1158/2159-8290.CD-12-0107

RESEARCH ARTICLE

CD36 Repression Activates a Multicellular Stromal Program Shared by High Mammographic Density and Tumor Tissues

Rosa Anna DeFilippis[1,2], Hang Chang[5], Nancy Dumont[1,2], Joseph T. Rabban[1], Yunn-Yi Chen[1], Gerald V. Fontenay[5], Hal K. Berman[6], Mona L. Gauthier[6], Jianxin Zhao[1,2], Donglei Hu[3], James J. Marx[7], Judy A. Tjoe[7], Elad Ziv[3], Maria Febbraio[8], Karla Kerlikowske[3,4], Bahram Parvin[5], and Thea D. Tlsty[1,2]

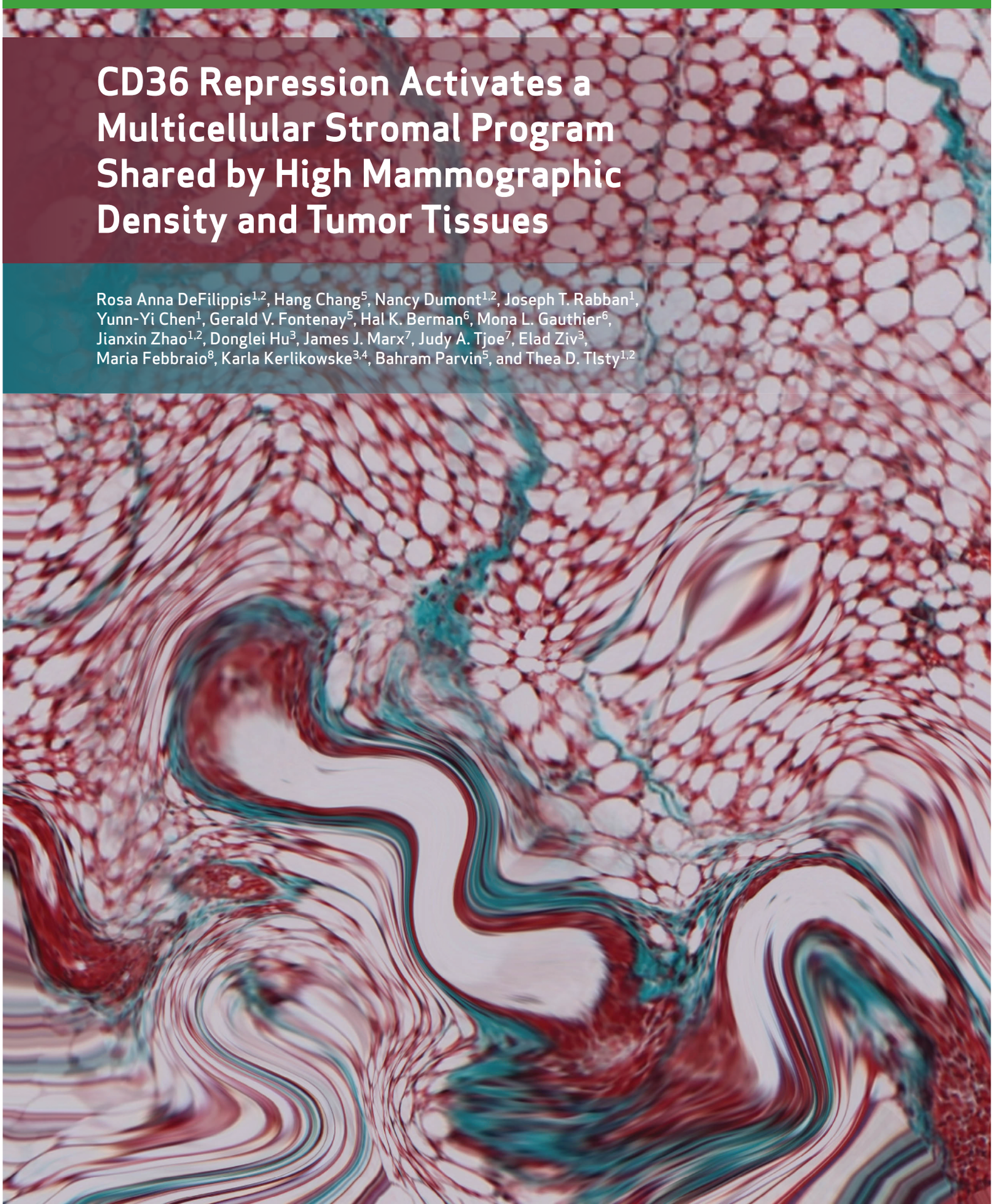

Published OnlineFirst July 9, 2012; DOI: 10.1158/2159-8290.CD-12-0107

ABSTRACT

Although high mammographic density is considered one of the strongest risk factors for invasive breast cancer, the genes involved in modulating this clinical feature are unknown. Tissues of high mammographic density share key histologic features with stromal components within malignant lesions of tumor tissues, specifically low adipocyte and high extracellular matrix (ECM) content. We show that CD36, a transmembrane receptor that coordinately modulates multiple protumorigenic phenotypes, including adipocyte differentiation, angiogenesis, cell–ECM interactions, and immune signaling, is greatly repressed in multiple cell types of disease-free stroma associated with high mammographic density and tumor stroma. Using both *in vitro* and *in vivo* assays, we show that CD36 repression is necessary and sufficient to recapitulate the above-mentioned phenotypes observed in high mammographic density and tumor tissues. Consistent with a functional role for this coordinated program in tumorigenesis, we observe that clinical outcomes are strongly associated with *CD36* expression.

SIGNIFICANCE: CD36 simultaneously controls adipocyte content and matrix accumulation and is coordinately repressed in multiple cell types within tumor and high mammographic density stroma, suggesting that activation of this stromal program is an early event in tumorigenesis. Levels of CD36 and extent of mammographic density are both modifiable factors that provide potential for intervention. *Cancer Discov; 2(9); 826–39. ©2012 AACR.*

INTRODUCTION

Many tissues are comprised of an epithelium associated with a stroma that is composed of extracellular matrix (ECM) proteins, adipocytes, fibroblasts, endothelial cells, neuronal cells, and immune cells. Fibroblasts, a major stromal cell type, produce many components of the ECM, as well as proteases that remodel it (1). In addition, fibroblast signaling is a critical determinant of epithelial and stromal cell fate during development and differentiation (2), tissue homeostasis, and wound healing (1).

Stromal changes associated with malignant lesions are heterogeneous and range from tumor suppressing to tumor promoting. Tumors, subtyped by marker expression in epithelial cells, can be further categorized by their stromal signature, which dictates good or poor outcome (3). Fibroblasts within the stroma of malignant lesions, called carcinoma-associated fibroblasts (CAF), differ from their counterparts in disease-free tissue (4). CAFs can stimulate tumor progression of initiated nontumorigenic epithelial cells, both *in vitro* and *in vivo*, whereas normal fibroblasts cannot (5). CAFs increase proliferation and decrease apoptosis in adjacent epithelial cells and promote angiogenesis by recruiting endothelial progenitor cells into tumors (5, 6). All other stromal components, including immune cells and endothelial cells, also participate in malignant progression (4).

The stroma within and immediately adjacent to a malignant lesion may exhibit a range of histologic alterations, called desmoplasia. The alterations range from a predominantly cellular stroma, containing fibroblasts, vascular cells, and immune cells with little ECM, to a dense tissue with a minimum of cells and a maximum content of matrix (4, 7). In addition, tumor stroma exhibits a reduction in the size and number of adipocytes (8). The most odious stromal changes include extreme ECM deposition and remodeling, along with aberrant vasculature and fibroblast and immune cell infiltration. Classically, participation of the stroma has been viewed as a reactive process, in which signals from malignant epithelial cells recruit and stimulate these stromal components.

Interestingly, some desmoplastic features are seen in cancer-free tissues of women at high risk for breast cancer, namely in the context of wound healing, radiation response, pregnancy-associated involution, and high mammographic density (4, 8–10). Mammographic density is of particular interest, as almost one third of breast cancers are thought to be attributable to phenotypes associated with high breast density, and mammographic density is a strong risk factor with high prevalence (11, 12). Mammographic density is determined by the relative amounts of radiolucent material (fat) and radiodense material (epithelial cells, fibroblasts, and connective tissue) within the breast on a mammogram, either of which may occupy anywhere between 0% and 100% of the gland. Radiodense areas exhibit several histologic characteristics of

Authors' Affiliations: [1]Department of Pathology, [2]Comprehensive Cancer Center, [3]Department of Medicine and [4]Departments of Epidemiology and Biostatistics, University of California San Francisco, San Francisco; [5]Lawrence Berkeley National Laboratory, Berkeley, California; [6]Department of Laboratory Medicine and Pathobiology, University of Toronto, Toronto, Ontario, Canada; [7]Department of Patient Centered Research, Division of Breast Oncology, Aurora Health Care, Milwaukee, Wisconsin; and [8]Department of Molecular Cardiology, Lerner Institute, Cleveland Clinic Foundation, Cleveland, Ohio

Note: Supplementary data for this article are available at Cancer Discovery Online (http://cancerdiscovery.aacrjournals.org/).

Corresponding Author: Thea D. Tlsty, Department of Pathology, Comprehensive Cancer Center, University of California San Francisco, 513 Parnassus, HSW 513, San Francisco, CA 94143. Phone: 415-502-6115; Fax: 415-502-6163; E-mail: Thea.Tlsty@ucsf.edu

doi: 10.1158/2159-8290.CD-12-0107

Published OnlineFirst July 9, 2012; DOI: 10.1158/2159-8290.CD-12-0107

stroma associated with malignant epithelial cells, specifically low adipocyte content and high ECM and stromal cell content (9, 10). Epidemiologic studies suggest that women with high mammographic density have a 4- to 6-fold increase in risk for invasive breast cancer compared with women with low mammographic density (11, 13–15).

Studies comparing pairs of monozygotic and dizygotic twins attributed 53% to 67% of the variation in mammographic density to heritable factors, with the remaining portion modulated by environmental or physiologic factors (16–21). For example, postmenopausal hormone therapy increases mammographic density in some women, whereas tamoxifen treatment decreases mammographic density in both pre- and postmenopausal women and subsequently modulates breast cancer risk (19, 21). This modulation by exogenous factors provides an exciting opportunity for intervention and prevention.

Boyd and colleagues examined the molecular composition of low and high mammographic density tissues (9, 10) and reported higher levels of insulin-like growth factor-I and tissue inhibitor of metalloproteinase 3 in high mammographic density tissue. Recent studies found additional changes including differences in estrogen and prostaglandin metabolism and TGF-β signaling (22–24). Although these studies begin to define the molecular constituents of mammographic density that may explain the basis of high mammographic density and its association with increased breast cancer risk, they are correlative and thus cannot show that these genes or proteins mechanistically modulate phenotypes of mammographic density.

The observation of multiple desmoplastic phenotypes in tissues of high mammographic density, in the absence of a tumor, strongly suggests that these stromal phenotypes are not simply part of a reactive response to existing tumor cells but also represent a program involving multiple stromal components that may create a proactive milieu for the emergence or progression of cancer. Therefore, we hypothesized that the phenotypes observed in both high mammographic density and tumor stroma may be controlled by a common molecular program and thus their stromal components would share phenotypic, molecular, and functional characteristics.

Here we show that the level of expression of a single molecule, CD36, is necessary and sufficient to simultaneously control adipocyte content and matrix accumulation, 2 phenotypes shared by desmoplasia and high mammographic density. CD36, a widely expressed transmembrane receptor, modulates cell type- and ligand-specific phenotypes, including adipocyte differentiation, angiogenesis, apoptosis, TGF-β activation, cell–ECM interactions, and immune signaling (25). We found that CD36 expression was negligible in multiple cell types of tumor stroma compared with surrounding histologically disease-free tissue. Strikingly, high mammographic density tissues, devoid of any malignancy, also showed reduced CD36 levels in multiple cell types compared with low mammographic density tissues. The low level of CD36 expression shared by high-risk (but cancer-free) and malignant tissues suggests that it constitutes a causal and very early event in generating the distinctive characteristics of tumor stroma.

RESULTS

Desmoplasia and Tissues with High Mammographic Density Share Histologic Characteristics

The appearance of stroma associated with malignant epithelial cells is strikingly different from the appearance of most stroma associated with disease-free ductal tissue. Increases in ECM, endothelial and immune components, and the absence of adipocytes are obvious upon inspection (Fig. 1). Strikingly, similar stromal alterations are observed histologically in disease-free tissue of women with high mammographic density as compared with women with low mammographic density, specifically low adipocyte and high ECM content (Fig. 1). We examined fibroblasts from tissue of high and low mammographic density, as well as from tumor tissue, for phenotypic similarities that may underlie their shared histologic appearance.

HDAFs and LDAFs Recapitulate Phenotypes of High and Low Mammographic Density Tissues, Respectively, *In Vitro*

To determine whether fibroblasts obtained from low and high mammographic density tissues and propagated *in vitro* could recapitulate the 2 prominent *in vivo* phenotypic differences described above, low-density associated fibroblasts (LDAF) and high-density associated fibroblasts (HDAF) were purified from disease-free breast biopsies from women with 25% to 50% mammographic density and women with more than 75% mammographic density, respectively (Supplementary Table S1). LDAFs and HDAFs were placed under proliferative or adipocyte differentiation conditions for 6 days

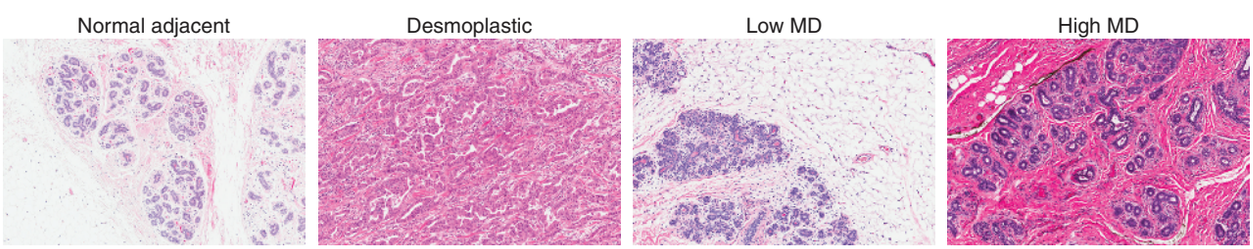

Figure 1. Desmoplasia and tissues with high mammographic density share histologic characteristics. Representative bright field images (original magnification ×5) of paraffin sections stained with hematoxylin and eosin (nuclei: blue, ECM: pink, adipocytes: white). Left: desmoplastic tissue and histologically normal adjacent tissue from a patient with invasive ductal carcinoma. Right: cancer-free tissue from one woman with low mammographic density and one woman with high mammographic density. MD, mammographic density.

Published OnlineFirst July 9, 2012; DOI: 10.1158/2159-8290.CD-12-0107

before assessing their ability to accumulate fat by Oil Red O staining (Fig. 2A). Fat accumulation was quantitated on a cell-by-cell basis as previously described (Supplementary Fig. S1; ref. 26). This analysis showed that, although both LDAFs and HDAFs accumulated fat under differentiation conditions (10.0-fold and 5.6-fold, respectively, $P < 10^{-8}$), HDAFs accumulated significantly less fat (3.1-fold, $P < 10^{-8}$) than LDAFs (Fig. 2B). This decrease in the average amount of fat accumulation per cell was due to a decrease in both the percentage of cells that contain fat and the amount of fat per cell (Supplementary Fig. S2).

To determine whether LDAFs and HDAFs differed in their adipocyte differentiation capacity, rather than simply fat storage, the expression levels of *CD36* and *leptin* (*LEP*; previously reported to be upregulated during adipocyte differentiation; ref. 27) were measured by quantitative PCR (QPCR) in cells grown under proliferative or adipocyte differentiation conditions for 2 weeks. Both LDAFs and HDAFs could undergo adipocyte differentiation; however, LDAFs showed higher levels of expression of *CD36* and *LEP* compared with HDAFs (*CD36*: 2.7-fold, $P = 0.03$; *LEP*: 6.8-fold, $P = 0.05$; Fig. 2C). These data showed that differences in fat accumulation between LDAFs and HDAFs are due to differences in their adipocyte differentiation capabilities.

Having shown that cultured LDAFs and HDAFs recapitulated their respective *in vivo* adipocyte phenotypes, we examined whether they could also recapitulate their *in vivo* matrix accumulation phenotypes in a short-term assay. LDAF and HDAF cultures were probed after 5 days of propagation for accumulation of matrix proteins known to be increased in desmoplasia: collagen 1A1 (COL1A1), fibronectin (FN1), osteopontin (OPN), and tenascin C (TNC; ref. 1; Supplementary Fig. S3). Cell-by-cell quantitative immunofluorescence analysis (Supplementary Fig. S1) revealed heterogeneity within the cultures with an overall small but statistically significant greater amount of COL1A1, FN1, and OPN (each 1.1-fold, $P < 10^{-8}$) in HDAFs compared with LDAFs (Fig. 2D). However, HDAFs accumulated a statistically significant lesser amount of TNC (1.1-fold, $P < 10^{-8}$) than LDAFs, suggesting that there is not a global increase in all matrix protein accumulation (Fig. 2D). One could speculate that this modest increase in matrix accumulation over a prolonged period of time (years), in contrast to our 5-day assay, could account for the dramatic differences observed *in vivo*.

CAFs Recapitulate Phenotypes of Desmoplasia *In Vitro*

CAFs have been shown to promote ECM deposition *in vitro* and *in vivo*, but little is known about their ability to modulate adipocyte differentiation (1). To this end, human mammary fibroblasts purified from invasive cancer tissues (CAFs) and from reduction mammoplasty tissues (RMF; Supplementary Table S2) were assayed as above for fat accumulation (Fig. 2E, left panel). Cell-by-cell quantitation of Oil Red O staining (Supplementary Fig. S1) showed that, although both RMFs and CAFs accumulated fat under differentiation conditions (27-fold and 8-fold, respectively, $P < 10^{-8}$), CAFs were deficient in fat accumulation compared with RMFs (5.8-fold, $P < 10^{-8}$; Fig. 2E, right panel).

CD36 Expression Is Decreased in Fibroblasts from High Mammographic Density and Tumor Tissues

To gain insight into the molecular basis for these phenotypes, gene expression profiling was used to identify genes differentially expressed between LDAFs and HDAFs (GEO GSE38506). *CD36* showed the largest difference, its expression being downregulated 3.7- to 4.3-fold in HDAFs relative to LDAFs (Supplementary Table S3). To validate these microarray results, CD36 transcript and protein levels were measured in LDAFs and HDAFs by QPCR and Western blot analysis. Both CD36 gene expression (8.6-fold, $P = 0.002$) and protein levels were decreased in HDAFs relative to LDAFs (Fig. 3A and B).

Given the striking downregulation of *CD36* in fibroblasts of high mammographic density, we examined *CD36* expression in fibroblasts isolated from malignant tissue and in microarrays of tumor tissue. *CD36* expression, measured by QPCR, was decreased 4.3-fold ($P = 0.001$) in CAFs relative to RMFs (Fig. 3C). Similarly, analysis of 6 independent public gene expression datasets (Supplementary Table S4) consistently showed a statistically significant decrease in *CD36* expression in invasive ductal carcinoma (IDC) tissues compared with normal tissues (3.6- to 12.3-fold). In light of the striking repression of *CD36* in fibroblasts from high mammographic density and tumor tissues, we examined the role of *CD36* in modulating the 2 prominent *in vivo* phenotypes shared by these tissues: decreased adipocyte content and increased matrix accumulation (4, 8–10).

CD36 Expression Is Necessary and Sufficient to Modulate Adipocyte Differentiation and Matrix Accumulation *In Vitro*

Little is known about the basis of decreased adipocyte content in high mammographic density and desmoplastic tissues. However, induction of *CD36* expression is necessary for proper adipocyte differentiation in preadipocytes (28) and serves as a marker for terminal differentiation (27). To determine whether *CD36* expression could modulate adipocyte content, we genetically modulated *CD36* levels in RMFs selected for their intermediate baseline expression level of *CD36*. To determine whether *CD36* expression was necessary for fat accumulation, *CD36* expression was repressed in RMFs by transduction of lentiviral particles expressing short hairpin RNA to *CD36* (shCD36; Supplementary Fig. S4). Cell-by-cell quantitation of Oil Red O staining (Supplementary Fig. S1) showed that although both control (shLuc) and shCD36 cells accumulated fat under differentiation conditions (8.9-fold and 3.1-fold, respectively, $P < 10^{-8}$), control cells accumulated significantly more fat than shCD36 cells (6.1-fold, $P < 10^{-8}$; Fig. 4A). These data showed that *CD36* is necessary for fat accumulation. To determine whether *CD36* expression was sufficient for fat accumulation, *CD36* expression was increased in RMFs by transduction of lentiviral particles expressing *CD36* (CD36 OE; Supplementary Fig. S4). Cell-by-cell quantitation of Oil Red O staining (Supplementary Fig. S1) showed that, although both control (vector) and CD36 OE cells accumulated fat under differentiation conditions (2.2-fold and 4.7-fold, respectively, $P < 10^{-8}$), CD36 OE

Published OnlineFirst July 9, 2012; DOI: 10.1158/2159-8290.CD-12-0107

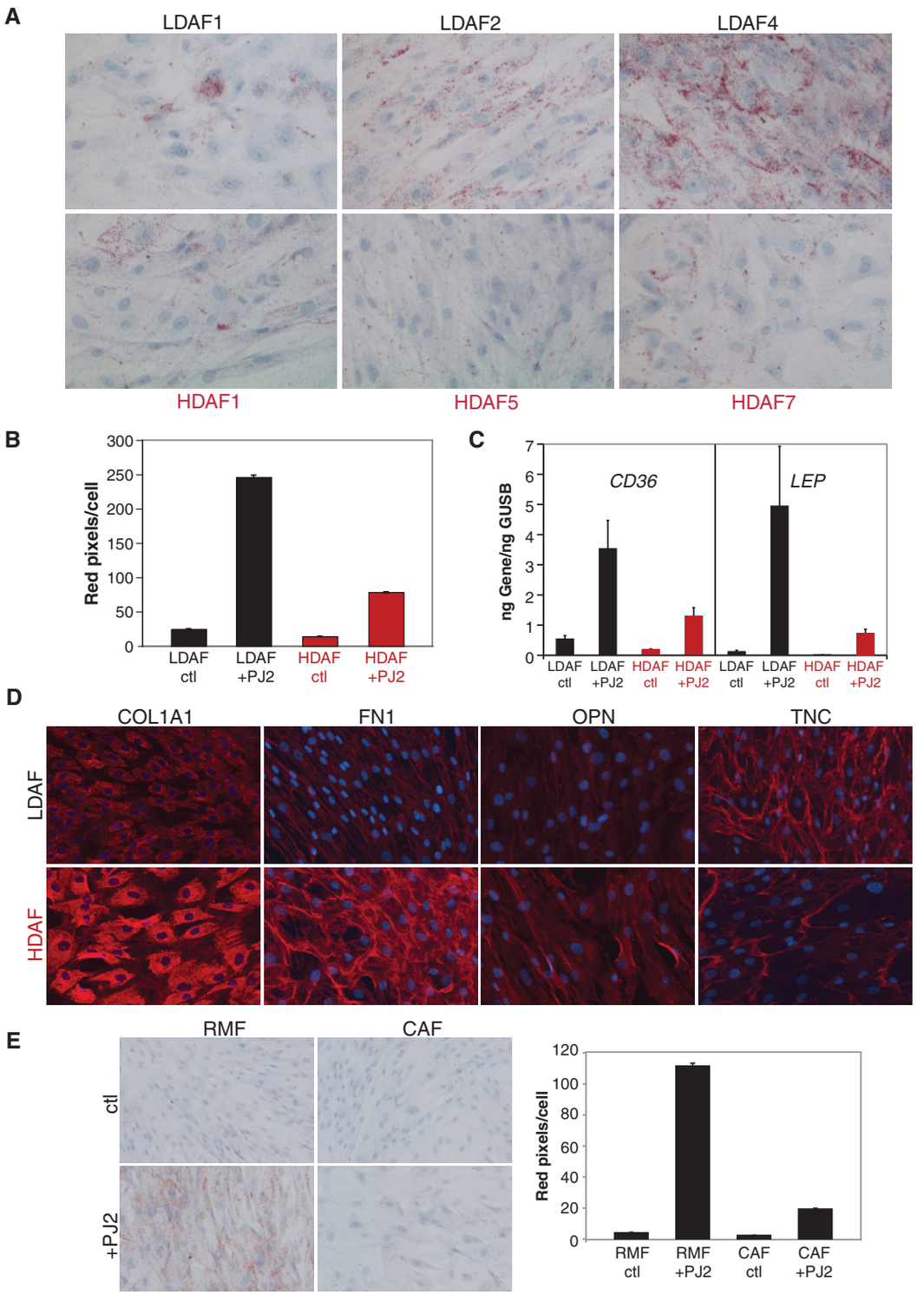

Figure 2. Cultured fibroblasts recapitulate multiple phenotypes associated with their respective tissues of origin. **A,** three LDAFs and 3 HDAFs were placed under proliferative (ctl) or adipocyte differentiation (+PJ2) conditions for 6 days and assessed for fat accumulation by Oil Red O staining. Representative bright field images (original magnification ×10) of the fibroblasts under differentiation conditions. **B,** average and SEM of Oil Red O staining per cell. **C,** four LDAFs and 4 HDAFs were placed under proliferative (ctl) or adipocyte differentiation conditions (+PJ2) for 2 weeks and assessed for adipocyte differentiation by measuring the expression of genes upregulated in adipogenesis. Average and SEM of *CD36* and *LEP* expression by QPCR ($n = 4$ for each of 4 LDAFs and 4 HDAFs). GUSB, beta-D-glucuronidase. **D,** representative fluorescent images (original magnification ×10) highlighting differential ECM protein deposition in 6 LDAFs and 6 HDAFs grown for 5 days and assessed for accumulation of matrix proteins COL1A1, FN1, OPN, and TNC. **E,** left: representative bright field images (original magnification ×10) of 1 RMF and 2 CAFs under proliferative (ctl) or adipocyte differentiation (+PJ2) conditions for 7 days and assessed for adipocyte formation by Oil Red O staining. Right: average and SEM of Oil Red O staining per cell.

Published OnlineFirst July 9, 2012; DOI: 10.1158/2159-8290.CD-12-0107

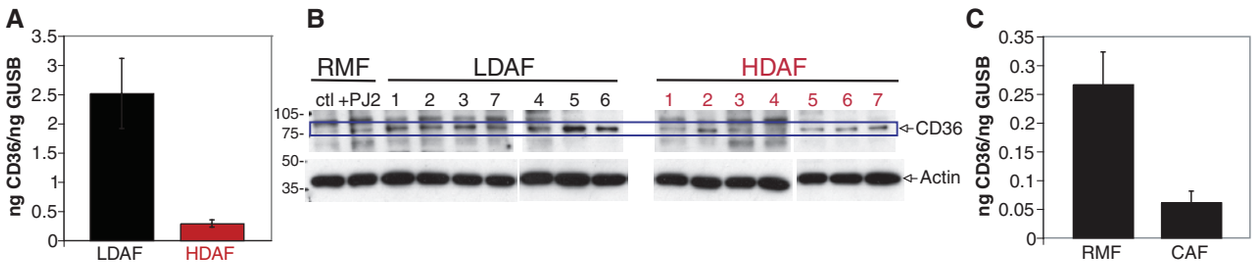

Figure 3. CD36 expression is decreased in HDAFs and CAFs relative to LDAFs and RMFs, respectively. **A,** average and SEM of *CD36* expression measured by QPCR ($n = 3$ for each of the 7 LDAFs and 7 HDAFs). **B,** Western blot analyses for CD36 (top), where the arrows indicate CD36 glycosylated state and actin (bottom). Positive control for CD36 expression: RMF under proliferative (ctl) or adipocyte differentiation (+PJ2) conditions for 7 days. **C,** average and SEM of *CD36* expression measured by QPCR ($n = 3$ for each of the 8 RMFs and 8 CAFs).

cells accumulated significantly more fat than control cells (3.3-fold, $P < 10^{-8}$; Fig. 4B). These data showed that *CD36* is sufficient for fat accumulation. Therefore, the decrease in *CD36* expression in HDAFs and CAFs could account for their reduced ability to accumulate fat compared with LDAFs and RMFs, respectively.

To determine whether *CD36* expression could also modulate matrix accumulation, the fibroblasts with genetically modulated levels of *CD36* described above were probed for the accumulation of matrix proteins known to be increased in HDAFs: COL1A1, FN1, and OPN (Fig. 4C). Cell-by-cell quantitative immunofluorescence analysis

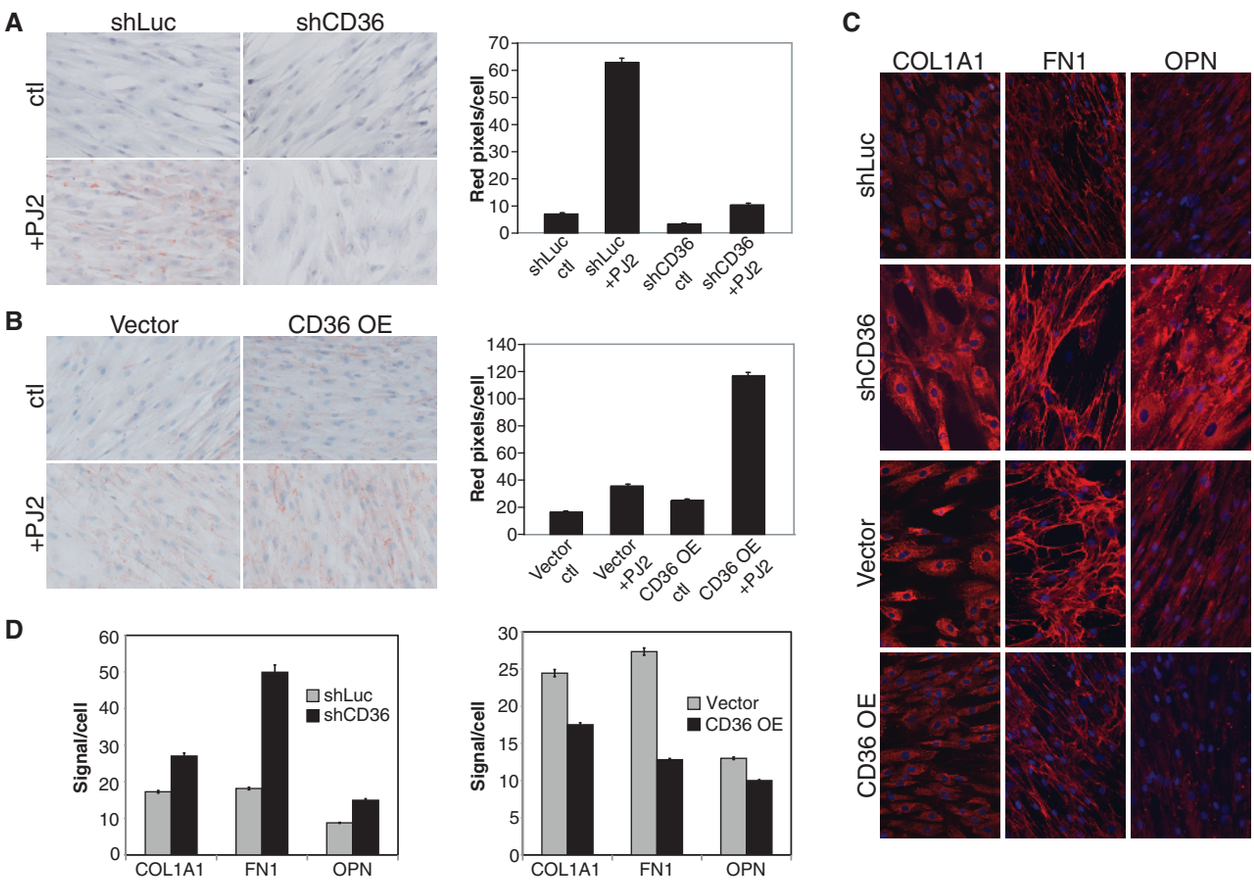

Figure 4. CD36 expression is necessary and sufficient to modulate adipocyte differentiation and matrix accumulation *in vitro*. **A** and **B,** left: Representative bright field images (original magnification ×10) of shLuc, shCD36, vector, or CD36 OE cells, under proliferative (ctl) or adipocyte differentiation (+PJ2) conditions for 7 days and assessed for adipocyte formation by Oil Red O staining. **A** and **B,** right: Average and SEM of Oil Red O staining per cell. **C,** representative fluorescent images (original magnification ×10) of shLuc, shCD36, vector, and CD36 OE cells grown for 5 days and assessed for accumulation of matrix proteins COL1A1, FN1, and OPN. **D,** average and SEM of staining per cell expressed as signal $\times 10^4$.

Published OnlineFirst July 9, 2012; DOI: 10.1158/2159-8290.CD-12-0107

(Supplementary Fig. S1) revealed that cells with low *CD36* (shCD36) accumulated a statistically significant greater amount of COL1A1, FN1, and OPN (1.6-fold, 2.8-fold, and 1.7-fold, respectively, $P < 10^{-8}$) compared with control cells (shLuc; Fig. 4D, left panel). Conversely, cells with high *CD36* (CD36 OE) accumulated a statistically significant lesser amount of COL1A1, FN1, and OPN (1.4-fold, 2.1-fold, and 1.3-fold, respectively, $P < 10^{-8}$) compared with control cells (vector; Fig. 4D, right panel). Of particular note, these changes in matrix accumulation were already observed after only 5 days of culture. These data showed that reduced *CD36* expression is necessary and sufficient for increased matrix accumulation. Taken together, the decreased *CD36* expression seen in high mammographic density and tumor tissues can result in the coordinated decrease in fat accumulation and increase in matrix accumulation observed *in vivo*.

Cd36 Knockout Mice Phenocopy Human High Mammographic Density and Desmoplastic Tissues

To determine whether the modulation of fat and matrix accumulation by *CD36*, which we observed *in vitro,* also occurs *in vivo*, we compared characteristics of fat and matrix accumulation in mammary glands of wild type (WT) and *Cd36* knockout (CD36 KO) mice (29). Paraffin sections of the #4 mammary glands of WT or CD36 KO mice were stained with Masson Trichrome, imaged (Fig. 5A) and quantitated on a cell-by-cell (for fat analysis) or image-by-image (for matrix analysis) basis (Supplementary Fig. S1). CD36 KO mice exhibited a statistically significant decrease (1.2-fold, $P < 10^{-8}$) in fat accumulation (fat cell area; Fig. 5B) and a statistically significant increase (2.1-fold, $P < 10^{-8}$) in matrix accumulation (Fig. 5C) relative to WT mice. Paraffin sections were stained for COL1A1 and FN1 (Fig. 5D and E, left panels), 2 matrix proteins modulated by *CD36 in vitro* (Fig. 4C and D). Image-by-image quantitative analysis (Supplementary Fig. S1) revealed that CD36 KO mice accumulated a statistically significant greater amount of COL1A1 and FN1 (both 1.6-fold, $P < 10^{-8}$ and $P = 5.5 \times 10^{-7}$, respectively) compared with WT mice (Fig. 5D and E, right panels). Therefore CD36 KO mice exhibited 2 prominent phenotypes of high mammographic density and desmoplastic tissues in women: decreased fat accumulation and increased matrix accumulation, showing causality between CD36 expression and modulation of both phenotypes *in vitro* and *in vivo*.

CD36 Expression Is Decreased in Multiple Cellular Compartments of High Mammographic Density Tissues Compared with Low Mammographic Density Tissues

CD36 is expressed on the surface of many cells that reside within tissue stroma, but not on epithelial cells (25). Given that microarray analysis of whole tumor tissues showed a dramatic reduction in CD36 compared with disease-free tissues (Supplementary Table S4), we determined whether cellular components other than fibroblasts also exhibited a repression of CD36. Tissue sections from core or excisional biopsies, obtained from cancer-free women with either low mammographic density or with high mammographic density (Supplementary Table S5) were stained for CD36 (Supplementary Fig. S5) and imaged (Fig. 6A, left panels). As expected, adipocytes, endothelial cells, macrophages, and fibroblasts each stained positive for CD36, whereas epithelial cells did not. However, a striking decrease in the intensity of CD36 staining in the high mammographic density tissues was observed in every cell type noted above, indicating that CD36 repression reflects a widespread multicellular program. CD36-positive staining was measured on a cell-by-cell basis as previously described (ref. 26; Supplementary Fig. S1). The average amount of CD36 staining per cell was lower in high mammographic density tissues compared with low mammographic density tissues (4.5-fold, $P < 10^{-8}$; Fig. 6A, right panel) due to a decrease in both the percentage of CD36-positive cells and the intensity of CD36 staining per cell (Supplementary Fig. S6).

CD36 Expression Is Decreased in Multiple Cell Types within the Stroma of Malignant Lesions Compared with Histologically Normal Adjacent Tissues

Having observed that CD36 expression is decreased in multiple cell types within tissues of high mammographic density, we investigated whether the same would be true in tumor tissues obtained from women with estrogen receptor (ER)/progesterone receptor (PR)-positive, HER2-positive, or ER/PR/HER2-negative (triple negative) IDC (Supplementary Table S6). Tissue sections from this cohort were stained for CD36 and imaged in both the tumor field and the histologically normal adjacent areas (Fig. 6B). In all tumor subtypes, CD36 expression was strikingly absent in the tumor field compared with the normal adjacent tissue (Fig. 6B). Cell-by-cell quantitation of CD36 staining (Supplementary Fig. S1) revealed that CD36 expression was reduced 14.7-fold ($P < 10^{-8}$) in tumor tissue compared with normal adjacent tissue (Supplementary Fig. S7). This was due to a decrease in both the percentage of CD36-positive cells and the intensity of CD36 staining per cell (Supplementary Fig. S6). A similar dramatic decrease in CD36 expression was observed in each tumor subtype (Fig. 6C). Notably, it has been reported that women with high mammographic density have a higher propensity to develop ER-negative tumors compared with women with low mammographic density (30). Strikingly, normal adjacent tissue from triple negative (ER-negative) tumors exhibited significantly lower levels of CD36 expression compared with ER-positive or HER2-positive tumors (Fig. 6C). Taken together, these data suggested that low expression levels of CD36, as seen in tissues with high mammographic density, might predispose a subset of women to develop triple negative tumors, a tumor subtype associated with poor disease outcome.

To identify the cellular basis of the reduced CD36 staining, we examined the cells that typically express CD36 in histologically normal tissues (adipocytes, endothelial cells, and macrophages). Although scarce, adipocytes within tumor tissue not only showed decreased expression of CD36 but were also smaller in size compared with adipocytes adjacent to the tumor (Supplementary Fig. S7). Staining of serial sections for endothelial and macrophage markers CD31 and CD68, respectively, revealed that

Published OnlineFirst July 9, 2012; DOI: 10.1158/2159-8290.CD-12-0107

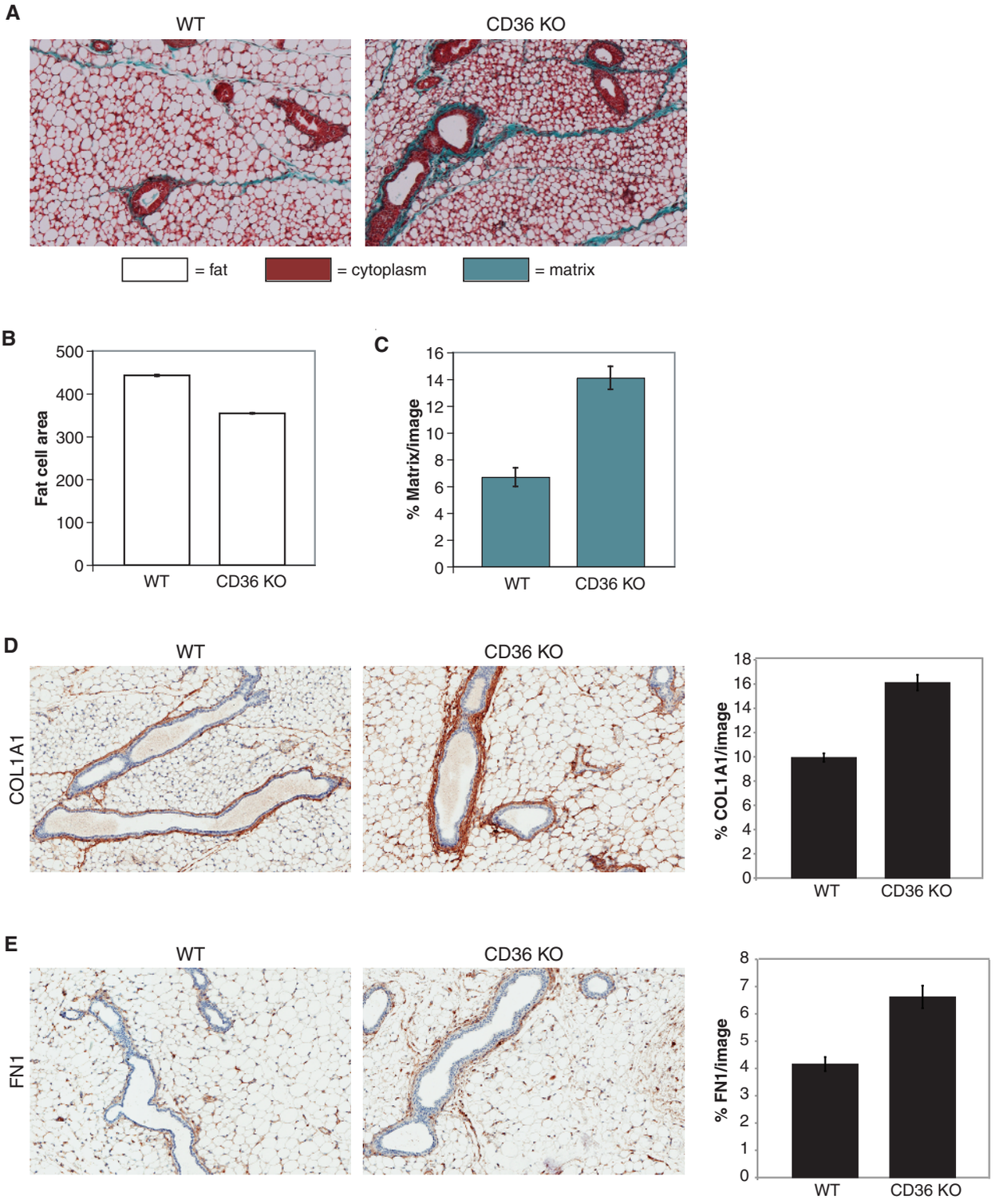

Figure 5. *CD36* knockout mice phenocopy human high mammographic density and desmoplastic tissues. Representative bright field images (original magnification ×10) of #4 mammary gland paraffin sections from either WT ($n = 7$) or CD36 KO ($n = 5$) mice stained with Masson Trichrome (**A**), or for COL1A1 (**D,** left) and FN1 (**E,** left). Average and SEM of fat cell area (**B**) or percent area of either matrix staining (**C**), COL1A1 staining (**D,** right) or FN1 staining (**E,** right).

Published OnlineFirst July 9, 2012; DOI: 10.1158/2159-8290.CD-12-0107

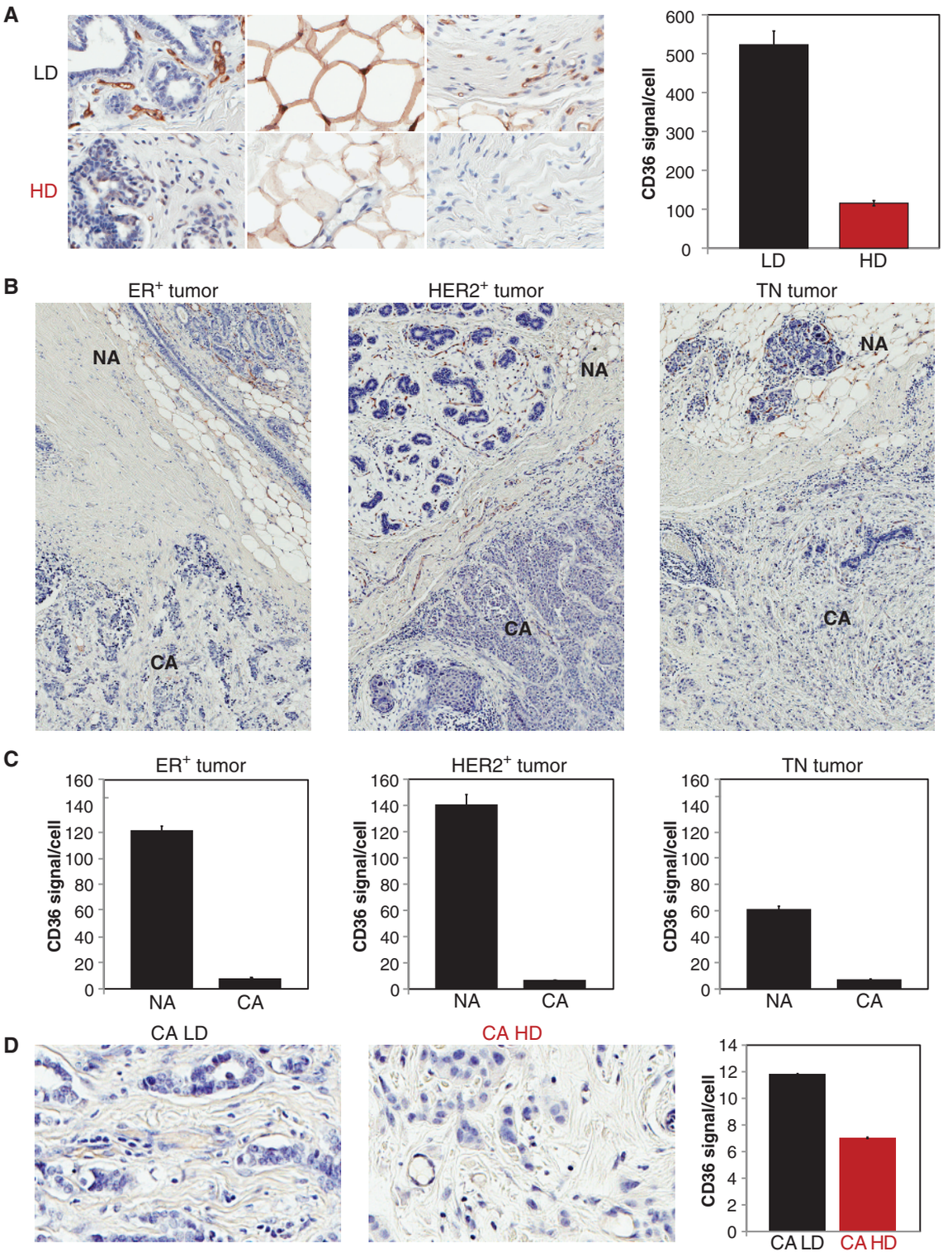

Figure 6. *CD36* expression is coordinately regulated in multiple cellular compartments. **A,** left: representative bright field images (original magnification ×20) of paraffin sections from 13 low mammographic density and 14 high mammographic density tissues stained for CD36. Right: average and SEM of CD36 signal per cell. **B,** representative bright field images (original magnification ×5) of paraffin sections with tumor and normal adjacent tissue from 8 ER-positive tumors, 6 HER2-positive tumors, and 6 triple negative tumors stained for CD36. **C,** average and SEM of CD36 signal per cell for each tumor subtype. **D,** left: representative bright field images (original magnification ×20) of paraffin sections from 21 low mammographic density and 14 high mammographic density ER-positive IDC patients stained for CD36. Right: average and SEM of CD36 signal per cell. CA, tumor; HD, high mammographic density; LD, low mammographic density; NA, normal adjacent, TN, triple negative.

Published OnlineFirst July 9, 2012; DOI: 10.1158/2159-8290.CD-12-0107

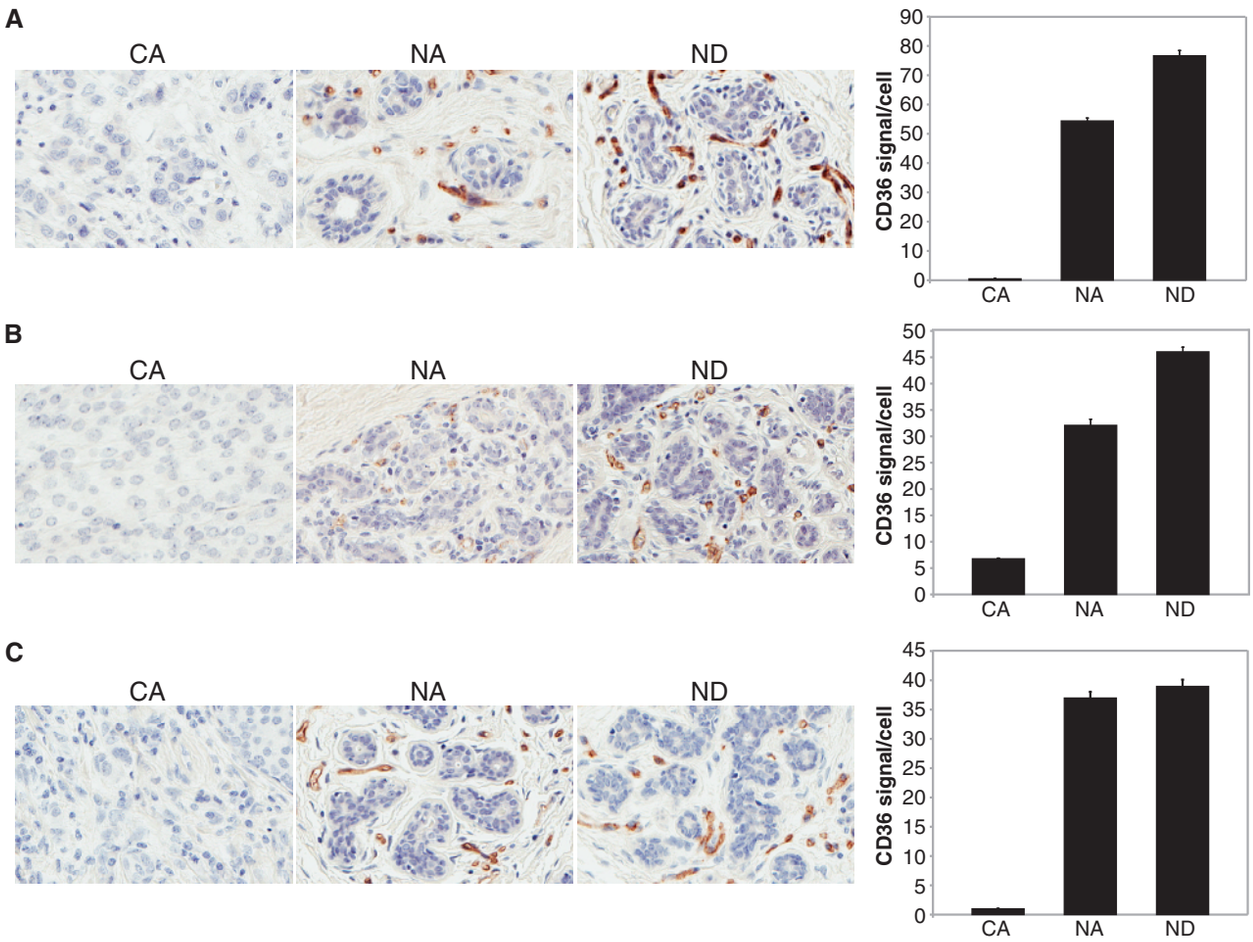

Figure 7. CD36 expression in tissue adjacent and distal to the tumor. **A–C,** left: representative bright field images (original magnification ×20) of paraffin sections with tumor and normal adjacent tissue or with normal distal tissue from 3 mastectomies stained for CD36. Right: average and SEM of CD36 signal per cell. CA, tumor; NA, normal adjacent; ND, normal distal.

endothelial cells and macrophages were still present within the field of tumor tissue, albeit with repressed CD36 expression (Supplementary Fig. S7). In contrast, in the normal adjacent tissue, endothelial cells and macrophages positive for CD31 and CD68, respectively, also stained positive for CD36 (Supplementary Fig. S7). Together with the results in Fig. 3C, these data showed that CD36 expression is actively repressed in fibroblasts, adipocytes, endothelial cells, and macrophages within tumor tissue compared with normal adjacent tissue. This documents that CD36 repression in tumor tissue, also seen in high mammographic density tissue, reflects a widespread, coordinated, and multicellular program.

The repression of CD36 in multiple cell types in high mammographic density tissue compared with low mammographic density tissue, in the absence of a tumor, suggests that this repression can be an early event that precedes overt tumor formation. If this were the case, one might predict that CD36 levels would be repressed in histologically normal tissue directly adjacent to the tumor compared with histologically normal tissue distal to the tumor. To test this hypothesis, multiple tissue sections containing both tumor and histologically normal adjacent tissue or histologically normal distal tissue (>40 mm away from the tumor) were obtained from 3 women with invasive cancer (Supplementary Table S7 and Fig. S8). Tissue sections were stained for CD36, imaged in the tumor, normal adjacent, and normal distal fields (Fig. 7A–C, left panels) and quantified for CD36 expression on a cell-by-cell basis (Supplementary Fig. S1). In accordance with the results reported above, CD36 expression was reduced in the tumor compared with normal adjacent and normal distal tissues in all 3 women (4.7-fold to 113-fold and 6.8-fold to 159-fold, respectively, $P < 10^{-8}$; Fig. 7A–C, right panels). Consistent with the hypothesis above, we observed in 2 of 3 cases that the normal adjacent tissue exhibited CD36 repression compared with its matched normal distal tissue (1.4-fold, $P < 10^{-8}$; Fig. 7A and B). In further support of this interpretation, it has been reported that invasive cancers often develop in regions previously measured as radiodense for many years before tumor detection (31). Interestingly, one sample did not show this difference between normal adjacent and normal distal tissues (Fig. 7C).

Published OnlineFirst July 9, 2012; DOI: 10.1158/2159-8290.CD-12-0107

A more detailed analysis of this heterogeneity is currently under investigation.

Clinical Outcome Is Associated with *CD36* Expression

Given the dramatic universal repression of CD36 observed within the stroma of all tumor subtypes examined (Fig. 6B and C), we determined whether the initial CD36 levels in non-diseased breast tissue (i.e., mammographic density) would stratify tumors for their ultimate CD36 repression and subsequent clinical phenotypes. Tissue sections containing tumor tissue obtained from women with low mammographic density and women with high mammographic density diagnosed with ER-positive IDC (Supplementary Table S8) were stained for CD36 and imaged (Fig. 6D, left panels). As expected, CD36 staining was very low in all tumor tissues. However, using cell-by-cell quantitation (Supplementary Fig. S1), the average amount of CD36 staining per cell was lower in the tumor tissues of women with high mammographic density compared with women with low mammographic density (1.7-fold, $P < 10^{-8}$; Fig. 6D, right panel). This was due to a decrease in both the percentage of CD36-positive cells and the intensity of CD36 staining per cell (Supplementary Fig. S6).

Women with high mammographic density who develop invasive cancer have an increased risk for aggressive disease, in that they develop larger tumors of more advanced stage and higher grade compared with women with low mammographic density (30, 32, 33). Because CD36 expression is reduced in tissues of high mammographic density, we examined whether *CD36* expression was correlated with tumor grade and size. We interrogated *CD36* expression in 2 public gene expression datasets (GSE6532 and GSE9195) for which molecular and associated clinical data were available for tumor samples from a total of 398 treatment-naive IDC patients (34, 35). We analyzed tumor grade, tumor size, and age as a function of *CD36* expression using linear regression analyses (Supplementary Table S9). For the purpose of this analysis, we transformed *CD36* levels so that they approximated a standard normal distribution (mean ~0, SD ~1). These analyses revealed a statistically significant inverse relationship between *CD36* expression and tumor grade and, independently, tumor size. *CD36* expression was reduced 0.38 SD ($P = 0.007$) in poorly differentiated tumors (grade 3) compared with well-differentiated tumors (grade 1), after adjusting for the association between *CD36* expression and tumor size. In addition, *CD36* expression was reduced 0.15 SD ($P = 0.003$) for every 1 cm increase in tumor size, after adjusting for the association between *CD36* expression and tumor grade. There was no significant association between *CD36* expression and age.

In sum, stromal characteristics before tumor formation, in this case reflected by extent of mammographic density and *CD36* expression levels, are associated with clinical outcome.

DISCUSSION

Using a combination of *in vitro* cell assays and *in vivo* screening of human and murine mammary tissue samples, we show that the level of expression of a single molecule, CD36, is necessary and sufficient to simultaneously control adipocyte content and matrix accumulation, 2 phenotypes that histologically define mammographic density. This is the first report of a gene shown to mechanistically modulate selected phenotypes of mammographic density. An important and novel finding of our study is that repression of CD36 is observed in both stroma associated with a malignant lesion and in breast tissue with high mammographic density in the absence of malignancy. Equally important is our demonstration that repression of CD36 is not limited to a specific cell type but rather is observed in all stromal components, as documented here for adipocytes, endothelial cells, macrophages, and fibroblasts, thus highlighting that expression of CD36 is part of a complex, coordinated, multicellular program. Taken together, these data suggest that expression of this stromal program is not only a reactive response to existing tumor cells but also represents a physiologic state that increases cancer risk. Our data suggest a functional role for this coordinated program because the more repressed CD36 expression is, the more aggressive the tumor.

CD36 is uniquely poised to coordinately orchestrate distinct protumorigenic phenotypes involving multiple cell types. In endothelial cells, in which CD36 blocks VEGF-induced proliferation, migration, and sprouting as well as induces apoptosis in response to ligand binding, its reduced expression could promote a proangiogenic phenotype (36, 37). In activated macrophages, in which CD36 promotes the formation of foam cells and atherosclerotic plaques, triggers the release of inflammatory cytokines and reactive oxygen species (ROS), and inhibits migration (25), its reduced expression could induce multiple, potentially protumorigenic, phenotypes. In support of this, macrophages from CD36 KO mice have reduced levels of ROS, iNOS, and inflammatory cytokines (including IFN-γ and TNF-α) and increased arginase activity (38), indicative of a shift from an M1 proinflammatory/antitumorigenic state to an M2 anti-inflammatory/protumorigenic state (39). In dendritic cells, in which CD36 normally mediates the uptake of apoptotic cells and the cross-presentation of tumor-specific antigens to cytotoxic T cells (25), its reduced expression could allow the tumor to evade the immune system (40). The decreased adipocyte differentiation [with reduced adiponectin (*Apn*)] and increased matrix accumulation [with increased collagen (*Col1a1*)] that we observed with reduced *CD36* expression *in vitro* and *in vivo* have been shown to cause an increase in tumor burden, angiogenesis, and metastasis in a murine mammary tumor model (MMTV-PyMT mice crossed with *Apn* KO or *Col1a1*^{tmJae} mice, respectively; refs. 41, 42). Finally, increased matrix accumulation could stiffen the microenvironment, thereby potentially altering mechanosensory networks involved in differentiation and malignancy (43, 44). In light of the central role of CD36 in modulating many functions in multiple cell types, one would predict that the reduction of CD36 expression could have widespread consequences.

The pro-oncogenic tissue state created by repression of CD36 goes far beyond merely supporting the malignant program of a transformed epithelial cell; it creates an interactive

Published OnlineFirst July 9, 2012; DOI: 10.1158/2159-8290.CD-12-0107

milieu that actively participates in tumorigenesis. Hence, our study provides novel insights into a molecular program that controls several stromal phenotypes underlying tumorigenesis. The "single hit, multiple target" nature of CD36, similar to miRNAs, makes it a very attractive therapeutic target. Moreover, in light of its role in mammographic density, strategies to modulate CD36 have the potential to prevent cancer progression in women who are at high risk. In support of this, we show that increased expression of *CD36* can restore stromal phenotypes associated with low-risk tissues (Fig. 4). Promisingly, expression of CD36 can be increased *in vitro* by treatment with aspirin, dexamethasone, statins, or adalimumab and *in vivo* by treatment with tamoxifen (45–49). Finally, mammographic density can also be modulated by a variety of exogenous agents such as hormones, tamoxifen, and diet. As such, mammographic density represents a highly promising target for intervention as well as a biomarker that can assess response to prevention interventions (19, 21).

METHODS

Isolation and Propagation of Human Mammary Fibroblasts

Fibroblasts were isolated from reduction mammoplasty, low and high mammographic density, or tumor tissues and assessed for purity as described (5).

Microarray and Quantitative PCR Analysis

Total RNA, isolated from fibroblasts subjected or not to adipocyte differentiation, was used to generate cDNA using TaqMan Reverse Transcription Reagents (Applied Biosystems). The cDNA was used for QPCR (TaqMan) using the standard curve method with primer probe sets for *CD36* and *leptin*. Expression of *beta-D-glucuronidase (GUSB)* was used to normalize input cDNA. For microarray experiments, mRNA, amplified and biotinylated from total RNA obtained from LDAFs and HDAFs using the MessageAmp II Kit (Ambion), was fragmented and hybridized to HU133 plus 2 chips (Affymetrix).

Adipocyte Differentiation Assay

Fibroblasts, plated at near confluency and grown for 48 hours, were treated with 10 μmol/L 15-deoxy-$\Delta^{12,14}$-Prostaglandin J2 (PJ2; Cayman Chemical) to induce adipocyte differentiation. Lipid accumulation was assayed by Oil Red O staining. Adipocyte differentiation was assessed by monitoring *CD36* and *leptin* expression after 2 weeks of treatment.

Matrix Accumulation

Fibroblasts, plated at near confluency into 8-well glass chamber slides, were grown for 5 days. Matrix accumulation was assessed by monitoring expression of COL1A1 (Abcam), FN1 (BD Biosciences), OPN (Abcam), and TNC (R&D) with primary antibodies all diluted 1:100.

Human and Mouse Tissue Preparation and Immunohistochemistry

Mouse sections (5 μm) were stained with Masson Trichrome using standard protocols. Human sections (4 μm) and mouse sections were subjected to antigen retrieval: microwaving in EDTA buffer (pH = 8.0) for 1 minute for CD36, incubation in Citrate buffer (pH = 6.0) at 80°C for 1 hour for CD31 and CD68, or microwaving in citrate buffer (pH = 6.0) for 10 minutes for COL1A1 and FN1. Sections were incubated for 1 hour with antibodies to CD36 (Sigma-Aldrich), CD31 (Dako), CD68 (Dako), COL1A1 (Abcam), or FN1 (Epitomics) diluted 1:100, 1:20, 1:200, 1:500, and 1:250, respectively. Human sections were incubated for 20 minutes with Primary Antibody Enhancer (Thermo Scientific). All sections were incubated for 30 minutes with HRP Polymer (Thermo Scientific) and 5 minutes with diaminobenzidine, and then counterstained in Mayer hematoxylin to visualize nuclei.

Analysis of Published Microarray Data

Microarray datasets GSE6532 and GSE9195 were analyzed using the robust multiarray average method (50). Expression values for each of the 5 *CD36* probe sets were centered by the median, then divided by the SD. Linear regression analyses were used to test the associations between the expression of each *CD36* probe set and tumor grade, tumor size, and age. Data from the probe set that were most strongly associated with tumor grade and tumor size are presented in Supplementary Table S9.

Detailed experimental procedures are included in Supplementary Materials and Methods.

Disclosure of Potential Conflicts of Interest

No potential conflicts of interest were disclosed.

Authors' Contributions

Conception and design: R.A. DeFilippis, N. Dumont, Y.-Y. Chen, H.K. Berman, K. Kerlikowske, T.D. Tlsty

Development of methodology: R.A. DeFilippis, H.K. Berman, M.L. Gauthier, J. Zhao, T.D. Tlsty

Acquisition of data (provided animals, acquired and managed patients, provided facilities, etc.): R.A. DeFilippis, J.T. Rabban, Y.-Y. Chen, M.L. Gauthier, J. Zhao, J.J. Marx, J.A. Tjoe, M. Febbraio, K. Kerlikowske, T.D. Tlsty

Analysis and interpretation of data (e.g., statistical analysis, biostatistics, computational analysis): R.A. DeFilippis, H. Chang, J.T. Rabban, Y.-Y. Chen, H.K. Berman, D. Hu, E. Ziv, K. Kerlikowske, B. Parvin

Writing, review, and/or revision of the manuscript: R.A. DeFilippis, N. Dumont, J.T. Rabban, Y.-Y. Chen, D. Hu, J.J. Marx, J.A. Tjoe, E. Ziv, M. Febbraio, K. Kerlikowske, B. Parvin, T.D. Tlsty

Administrative, technical, or material support (i.e., reporting or organizing data, constructing databases): R.A. DeFilippis, G.V. Fontenay, J. Zhao, J.A. Tjoe, E. Ziv, K. Kerlikowske

Study supervision: R.A. DeFilippis, Y.-Y. Chen, T.D. Tlsty

Acknowledgments

The authors thank members of the Tlsty laboratory, particularly Drs. Colleen Fordyce and Philippe Gascard, for thoughtful discussions, the Nikon Imaging Center (UCSF) for imaging support, and Dr. Alfred Au (UCSF), the breast surgeons (Aurora Health Care), and Carol Halliday, RN (Aurora Health Care), for providing tissue.

Grant Support

This work was supported by NIH/NCI PO1 CA107584 to T.D. Tlsty, K. Kerlikowske, E. Ziv, and B. Parvin (under LBNL contract No. DE-AC02-05CH11231), California Breast Cancer Research Program grant 14OB-0165 to T.D. Tlsty, and NIH/NCI U54 CA143803 to T.D. Tlsty and B. Parvin (UC Riverside).

Received March 12, 2012; revised June 28, 2012; accepted July 2, 2012; published OnlineFirst July 9, 2012.

Published OnlineFirst July 9, 2012; DOI: 10.1158/2159-8290.CD-12-0107

REFERENCES

1. Kalluri R, Zeisberg M. Fibroblasts in cancer. Nat Rev Cancer 2006;6:392–401.
2. Arendt LM, Rudnick JA, Keller PJ, Kuperwasser C. Stroma in breast development and disease. Semin Cell Dev Biol 2010;21:11–8.
3. Finak G, Bertos N, Pepin F, Sadekova S, Souleimanova M, Zhao H, et al. Stromal gene expression predicts clinical outcome in breast cancer. Nat Med 2008;14:518–27.
4. Tlsty TD, Coussens LM. Tumor stroma and regulation of cancer development. Annu Rev Pathol 2006;1:119–50.
5. Olumi AF, Grossfeld GD, Hayward SW, Carroll PR, Tlsty TD, Cunha GR. Carcinoma-associated fibroblasts direct tumor progression of initiated human prostatic epithelium. Cancer Res 1999;59:5002–11.
6. Orimo A, Gupta PB, Sgroi DC, Arenzana-Seisdedos F, Delaunay T, Naeem R, et al. Stromal fibroblasts present in invasive human breast carcinomas promote tumor growth and angiogenesis through elevated SDF-1/CXCL12 secretion. Cell 2005;121:335–48.
7. Walker RA. The complexities of breast cancer desmoplasia. Breast Cancer Res 2001;3:143–45.
8. Bing C, Trayhurn P. New insights into adipose tissue atrophy in cancer cachexia. Proc Nutr Soc 2009;68:385–92.
9. Guo YP, Martin LJ, Hanna W, Banerjee D, Miller N, Fishell E, et al. Growth factors and stromal matrix proteins associated with mammographic densities. Cancer Epidemiol Biomarkers Prev 2001;10:243–48.
10. Li T, Sun L, Miller N, Nicklee T, Woo J, Hulse-Smith L, et al. The association of measured breast tissue characteristics with mammographic density and other risk factors for breast cancer. Cancer Epidemiol Biomarkers Prev 2005;14:343–9.
11. Byrne C, Schairer C, Wolfe J, Parekh N, Salane M, Brinton LA, et al. Mammographic features and breast cancer risk: effects with time, age, and menopause status. J Natl Cancer Inst 1995;87:1622–9.
12. Kerlikowske K, Shepherd J, Creasman J, Tice JA, Ziv E, Cummings SR. Are breast density and bone mineral density independent risk factors for breast cancer? J Natl Cancer Inst 2005;97:368–74.
13. Boyd NF, Byng JW, Jong RA, Fishell EK, Little LE, Miller AB, et al. Quantitative classification of mammographic densities and breast cancer risk: results from the Canadian National Breast Screening Study. J Natl Cancer Inst 1995;87:670–5.
14. Cummings SR, Tice JA, Bauer S, Browner WS, Cuzick J, Ziv E, et al. Prevention of breast cancer in postmenopausal women: approaches to estimating and reducing risk. J Natl Cancer Inst 2009;101:384–98.
15. Ziv E, Tice J, Smith-Bindman R, Shepherd J, Cummings S, Kerlikowske K. Mammographic density and estrogen receptor status of breast cancer. Cancer Epidemiol Biomarkers Prev 2004;13:2090–5.
16. Boyd NF, Dite GS, Stone J, Gunasekara A, English DR, McCredie MR, et al. Heritability of mammographic density, a risk factor for breast cancer. N Engl J Med 2002;347:886–94.
17. Ursin G, Lillie EO, Lee E, Cockburn M, Schork NJ, Cozen W, et al. The relative importance of genetics and environment on mammographic density. Cancer Epidemiol Biomarkers Prev 2009;18:102–12.
18. Chlebowski RT, McTiernan A. Biological significance of interventions that change breast density. J Natl Cancer Inst 2003;95:4–5.
19. Cuzick J, Warwick J, Pinney E, Duffy SW, Cawthorn S, Howell A, et al. Tamoxifen-induced reduction in mammographic density and breast cancer risk reduction: a nested case-control study. J Natl Cancer Inst 2011;103:744–52.
20. El-Bastawissi AY, White E, Mandelson MT, Taplin SH. Reproductive and hormonal factors associated with mammographic breast density by age (United States). Cancer Causes Control 2000;11:955–63.
21. Greendale GA, Reboussin BA, Slone S, Wasilauskas C, Pike MC, Ursin G. Postmenopausal hormone therapy and change in mammographic density. J Natl Cancer Inst 2003;95:30–7.
22. Haakensen VD, Biong M, Lingjaerde OC, Holmen MM, Frantzen JO, Chen Y, et al. Expression levels of uridine 5′-diphospho-glucuronosyltransferase genes in breast tissue from healthy women are associated with mammographic density. Breast Cancer Res 2010;12:R65.
23. Yang WT, Lewis MT, Hess K, Wong H, Tsimelzon A, Karadag N, et al. Decreased TGFbeta signaling and increased COX2 expression in high risk women with increased mammographic breast density. Breast Cancer Res Treat 2010;119:305–14.
24. Vachon CM, Sasano H, Ghosh K, Brandt KR, Watson DA, Reynolds C, et al. Aromatase immunoreactivity is increased in mammographically dense regions of the breast. Breast Cancer Res Treat 2011;125:243–52.
25. Silverstein RL, Febbraio M. CD36, a scavenger receptor involved in immunity, metabolism, angiogenesis, and behavior. Sci Signal 2009;2:re3.
26. Chang H, DeFilippis RA, Tlsty TD, Parvin B. Graphical methods for quantifying macromolecules through bright field imaging. Bioinformatics 2009;25:1070–5.
27. Gregoire FM, Smas CM, Sul HS. Understanding adipocyte differentiation. Physiol Rev 1998;78:783–809.
28. Sfeir Z, Ibrahimi A, Amri E, Grimaldi P, Abumrad N. CD36 antisense expression in 3T3-F442A preadipocytes. Mol Cell Biochem 1999;192:3–8.
29. Febbraio M, Abumrad NA, Hajjar DP, Sharma K, Cheng W, Pearce SF, et al. A null mutation in murine CD36 reveals an important role in fatty acid and lipoprotein metabolism. J Biol Chem 1999;274:19055–62.
30. Yaghjyan L, Colditz GA, Collins LC, Schnitt SJ, Rosner B, Vachon C, et al. Mammographic breast density and subsequent risk of breast cancer in postmenopausal women according to tumor characteristics. J Natl Cancer Inst 2011;103:1179–89.
31. Pereira SM, McCormack VA, Hipwell JH, Record C, Wilkinson LS, Moss SM, et al. Localized fibroglandular tissue as a predictor of future tumor location within the breast. Cancer Epidemiol Biomarkers Prev 2011;20:1718–25.
32. Aiello EJ, Buist DS, White E, Porter PL. Association between mammographic breast density and breast cancer tumor characteristics. Cancer Epidemiol Biomarkers Prev 2005;14:662–8.
33. Kerlikowske K, Cook AJ, Buist DS, Cummings SR, Vachon C, Vacek P, et al. Breast cancer risk by breast density, menopause, and postmenopausal hormone therapy use. J Clin Oncol 2010;28:3830–7.
34. Loi S, Haibe-Kains B, Desmedt C, Wirapati P, Lallemand F, Tutt AM, et al. Predicting prognosis using molecular profiling in estrogen receptor-positive breast cancer treated with tamoxifen. BMC Genomics 2008;9:239.
35. Loi S, Haibe-Kains B, Desmedt C, Lallemand F, Tutt AM, Gillet C, et al. Definition of clinically distinct molecular subtypes in estrogen receptor-positive breast carcinomas through genomic grade. J Clin Oncol 2007;25:1239–46.
36. Primo L, Ferrandi C, Roca C, Marchio S, di Blasio L, Alessio M, et al. Identification of CD36 molecular features required for its *in vitro* angiostatic activity. FASEB J 2005;19:1713–5.
37. Jimenez B, Volpert OV, Crawford SE, Febbraio M, Silverstein RL, Bouck N. Signals leading to apoptosis-dependent inhibition of neovascularization by thrombospondin-1. Nat Med 2000;6:41–8.
38. Kennedy DJ, Kuchibhotla S, Westfall KM, Silverstein RL, Morton RE, Febbraio M. A CD36-dependent pathway enhances macrophage and adipose tissue inflammation and impairs insulin signalling. Cardiovasc Res 2011;89:604–13.
39. Sica A, Larghi P, Mancino A, Rubino L, Porta C, Totaro MG, et al. Macrophage polarization in tumour progression. Semin Cancer Biol 2008;18:349–55.
40. McDonnell AM, Robinson BW, Currie AJ. Tumor antigen cross-presentation and the dendritic cell: where it all begins? Clin Dev Immunol 2010;2010:539519.
41. Landskroner-Eiger S, Qian B, Muise ES, Nawrocki AR, Berger JP, Fine EJ, et al. Proangiogenic contribution of adiponectin toward mammary tumor growth in vivo. Clin Cancer Res 2009;15:3265–76.

Published OnlineFirst July 9, 2012; DOI: 10.1158/2159-8290.CD-12-0107

42. Provenzano PP, Inman DR, Eliceiri KW, Knittel JG, Yan L, Rueden CT, et al. Collagen density promotes mammary tumor initiation and progression. BMC Med 2008;6:11.
43. Engler AJ, Sen S, Sweeney HL, Discher DE. Matrix elasticity directs stem cell lineage specification. Cell 2006;126:677–89.
44. Levental KR, Yu H, Kass L, Lakins JN, Egeblad M, Erler JT, et al. Matrix crosslinking forces tumor progression by enhancing integrin signaling. Cell 2009;139:891–906.
45. Vinals M, Bermudez I, Llaverias G, Alegret M, Sanchez RM, Vazquez-Carrera M, et al. Aspirin increases CD36, SR-BI, and ABCA1 expression in human THP-1 macrophages. Cardiovasc Res 2005;66:141–9.
46. Matasic R, Dietz AB, Vuk-Pavlovic S. Dexamethasone inhibits dendritic cell maturation by redirecting differentiation of a subset of cells. J Leukoc Biol 1999;66:909–14.
47. Ruiz-Velasco N, Dominguez A, Vega MA. Statins upregulate CD36 expression in human monocytes, an effect strengthened when combined with PPAR-gamma ligands Putative contribution of Rho GTPases in statin-induced CD36 expression. Biochem Pharmacol 2004;67:303–13.
48. Boyer JF, Balard P, Authier H, Faucon B, Bernad J, Mazieres B, et al. Tumor necrosis factor alpha and adalimumab differentially regulate CD36 expression in human monocytes. Arthritis Res Ther 2007;9:R22.
49. Saibara T, Ogawa Y, Onishi S. Tamoxifen in early breast cancer. Lancet 1998;352:404.
50. Irizarry RA, Hobbs B, Collin F, Beazer-Barclay YD, Antonellis KJ, Scherf U, et al. Exploration, normalization, and summaries of high density oligonucleotide array probe level data. Biostatistics 2003;4:249–64.

Published OnlineFirst July 9, 2012; DOI: 10.1158/2159-8290.CD-12-0107

AACR American Association for Cancer Research

CANCER DISCOVERY

CD36 Repression Activates a Multicellular Stromal Program Shared by High Mammographic Density and Tumor Tissues

Rosa Anna DeFilippis, Hang Chang, Nancy Dumont, et al.

Cancer Discovery 2012;2:826-839. Published OnlineFirst July 9, 2012.